HIERARCHICAL MARKOVIAN MODELS FOR 3D COMPUTED TOMOGRAPHY IN NON DESTRUCTIVE TESTING APPLICATIONS

Ali Mohammad-Djafari and Lionel Robillard

Laboratoire des Signaux et Systèmes,
Unité mixte de recherche 8506 (CNRS-Supélec-UPS)
Supélec, Plateau de Moulon, 3 rue Joliot Curie, 91192 Gif-sur-Yvette, France
and
Groupe P1B, Systèmes dynamiques et traitement de l'information,
Électricité De France (EDF), Chatou, France

ABSTRACT

So as to detect and characterize potential defects in pipes, inspections are carried out with the help of non-destructive examination techniques (NDE) including X-or radiography. Should a defect be detected, one can be asked to prove the component still stands the mechanical constraints. In these cases of expertise, the use of a 3-D reconstruction processing technique can be very useful. One characteristic of such applications is that, in general the number and angles of projections are very limited and the data are very noisy, so the problem is severely ill posed. Hopefully, in these applications we know *a priori* the number and the types of materials in the object under the study and this is a great piece of prior information. In this work, we first propose a particular hierarchical Markov-Potts *a priori* model which takes into account for the specificity of the Non Destructive Technique (NDT) Computed Tomography (CT). Then, we give details of a Bayesian estimation computation based on MCMC and EM techniques. Finally, we show the performances of the proposed 3D CT reconstruction method with a very limited number and angles of projections and very low signal to noise ratio simulating from simulating data. These data have been obtained from very simple defects (cubic form) with acquisition conditions that are supposed to be representatives of real inspection in power plants.

1. INTRODUCTION

So as to detect and characterize potential defects in pipes, inspections are carried out with the help of non-destructive examination techniques (NDE) including X-or radiography. Should a defect be detected, one can be asked to prove the component still stands the mechanical constraints. In these cases of expertise, the use of a 3-D reconstruction processing technique can be very useful. In order to process the radiograms numerically, the films must be sampled and digitized. Before dealing with the reconstruction process, previous steps are required :

- a pre-processing phase for correction of potential misalignments between films,
- a calibration stage that converts the gray level (which convey non physical meaning) into crossed thickness.

For more details the reader is referred to [13]. The simplest forward model in CT is the line integration model:

$$g(\boldsymbol{s}_i) = \int_{L_i} f(\boldsymbol{r}) \ \mathrm{d}l_i \qquad (1)$$

where $\boldsymbol{r} = (x,y,z)$ is a voxel position, $\boldsymbol{s}_i$ is a detector position, L_i is a line connecting the X ray source position to the detector position $\boldsymbol{s}_i$ and $\mathrm{d}l_i$ is a unit element on this line. When discretized this equation becomes

$$\boldsymbol{g} = \boldsymbol{H}\boldsymbol{f} + \boldsymbol{\varepsilon} \qquad (2)$$

where, $\boldsymbol{f} = \{f(\boldsymbol{r}), \boldsymbol{r} \in \mathscr{R}\}$ is a vector containing the discretized voxel values of the object, $\boldsymbol{g} = \{g(\boldsymbol{s}_i), i = 1, \cdots, M\}$ is a vector containing the values of the projection data, $\boldsymbol{\varepsilon}$ is a vector representing the modeling and measurement errors and $\boldsymbol{H}$ is a huge dimensional matrix representing the discretized line integral operator.

One of the characteristics of such applications is that, in general the number and angles of projections are very limited and data are noisy. The problem is then severely ill posed and prior knowledge is needed to obtain satisfactory reconstruction results. There has been many works dealing with this inverse problem. The main tool has been the regularization approach where the solution is defined as the minimizer of a compound criterion

$$J(\boldsymbol{f}) = Q(\boldsymbol{g} - \boldsymbol{H}\boldsymbol{f}) + \lambda\Omega(\boldsymbol{f})$$

where λ is the regularization parameter and Q and Ω has to be chosen appropriately to reflect the prior knowledge on the noise and on the image. This criteria have also been interpreted as the maximum *a posteriori* (MAP) in the Bayesian estimation framework where $\exp[-Q(\boldsymbol{f})]$ represents the likelihood term and $\exp[-\lambda\Omega(\boldsymbol{f})]$ the prior probability law. This approach has been used with success in many applications (e.g. [1, 2, 3, 4, 5, 6, 7]). The main contributions of those works are in choosing appropriate regularization functional or equivalently appropriate prior probability laws for $\boldsymbol{f}$ to enforce some particular properties of the object such as smoothness, positivity or piecewise smoothness [4, 5, 8, 9].

The main specificity of NDT applications of CT is that, in these applications, we know *a priori* the number and the types of materials in the object under the test, for example mainly metal and air or metal, air and a composite material. So, we know *a priori* that the reconstructed object must be piecewise homogeneous, *i.e.,* the object must be composed of a limited number of compact homogeneous regions with a limited known type of materials. This prior information has not always been used optimally. The main originality and contribution of this paper is to propose a method which accounts for this specificity in an optimal way.

2. PROPOSED METHOD

In this work, we first propose a particular hierarchical Markov-Potts *a priori* model which takes into account this specificity of the NDT application of CT. Then, we show that many classical regularization techniques are particular cases of the proposed method. Indeed, in the proposed method, we obtain directly and simultaneously the reconstructed object and a segmentation results thanks to the mixture of Gaussian marginal prior law of the voxels. Then, we give details of a Bayesian estimation algorithm based on MCMC and EM techniques. Finally, we show the performances of the proposed 3D CT reconstruction method with a very limited number and angles of projections and very low signal to noise ratio simulating from simulating data. These data have been obtained from very simple defects (cubic form) with acquisition conditions that are supposed to be representatives of real inspection in power plants.

2.1 Forward model and likelihood

Using the forward model (2) and assuming the noise to be centered, white and Gaussian with the covariance matrix $\Sigma_\varepsilon = {\sigma_\varepsilon}^2 \boldsymbol{I}$, we have

$$p(\boldsymbol{g}|\boldsymbol{f}) = \mathcal{N}(\boldsymbol{H}\boldsymbol{f}, \Sigma_\varepsilon) \propto \exp\left[\frac{-1}{2{\sigma_\varepsilon}^2}\|\boldsymbol{g}-\boldsymbol{H}\boldsymbol{f}\|^2\right] \quad (3)$$

2.2 Prior models for the objects in NDT applications

In the following, we propose two prior models which try to account for the specificity of the NDT applications. The first one is based on a mixture of Gaussian (MoG) model:

$$p(f(\boldsymbol{r})) = \sum_k \pi_k \mathcal{N}(m_k, v_k) \quad (4)$$

which translates the fact that all the voxels of the images in NDT applications represent a finite number K of materials characterized by the parameters (m_k, v_k) and proportions π_k with $\sum_k \pi_k = 1$. However, we propose here to introduce a hidden variable $z(\boldsymbol{r})$ with $P(z(\boldsymbol{r}) = k) = \pi_k$ which gives us the possibility to write

$$p(f(\boldsymbol{r})|z(\boldsymbol{r}) = k) = \mathcal{N}(m_k, v_k), \quad k = 1, \cdots, K \quad (5)$$

which becomes equivalent to the MoG model if we assume that the hidden variables $z(\boldsymbol{r})$ for different positions $\boldsymbol{r}$ are independent. But, we want to account for another specificity of the NDT images which is the distribution of the voxels in compact homogeneous regions. This can be achieved by putting a Markovian model on the hidden variables $z(\boldsymbol{r})$:

$$p(z(\boldsymbol{r})|z(\boldsymbol{r}'), \boldsymbol{r}' \in \mathcal{V}(\boldsymbol{r})) \propto \exp\left[\alpha \sum_{\boldsymbol{r}' \in \mathcal{V}(\boldsymbol{r})} \delta(z(\boldsymbol{r}) - z(\boldsymbol{r}'))\right] \quad (6)$$

where the parameter α controls the mean size of those regions and $\mathcal{V}(\boldsymbol{r})$ represents the set of voxel positions in the neighborhood of $\boldsymbol{r}$. In this work, we consider the six nearest neighbor voxels for $\mathcal{V}(\boldsymbol{r})$.

If we note by $\boldsymbol{z} = \{z(\boldsymbol{r}), \boldsymbol{r} \in \mathcal{R}\}$, then we can also write

$$p(\boldsymbol{z}) \propto \exp\left[\alpha \sum_{\boldsymbol{r}} \sum_{\boldsymbol{r}' \in \mathcal{V}(\boldsymbol{r})} \delta(z(\boldsymbol{r}) - z(\boldsymbol{r}'))\right] \quad (7)$$

where $\boldsymbol{z}$ represents a segmentation image for $\boldsymbol{f}$.

If now, we assume that all the voxels $f(\boldsymbol{r})$ conditionally to $z(\boldsymbol{r})$ are independents, then we can write

$$\begin{aligned} p(\boldsymbol{f}|\boldsymbol{z}) &\propto \prod_k \prod_{\boldsymbol{r} \in \mathcal{R}_k} \exp\left[\frac{-1}{2v_k}|f(\boldsymbol{r}) - m_k|^2\right] \\ &\propto \prod_k \exp\left[\frac{-1}{2v_k}|\boldsymbol{f}_k - m_k\boldsymbol{1}|^2\right] \\ &\propto \prod_{\boldsymbol{r} \in \mathcal{R}} \exp\left[\frac{-1}{2v(\boldsymbol{r})}|f(\boldsymbol{r}) - m(\boldsymbol{r})|^2\right] \end{aligned}$$

where we used the notations $\mathcal{R}_k = \{\boldsymbol{r} : z(\boldsymbol{r}) = k\}$ and $\boldsymbol{f}_k = \{f(\boldsymbol{r}), \boldsymbol{r} \in \mathcal{R}_k\}$, $m(\boldsymbol{r}) = \{m_k, \boldsymbol{r} \in \mathcal{R}_k\}$, $v(\boldsymbol{r}) = \{v_k, \boldsymbol{r} \in \mathcal{R}_k\}$ and where $\cup_k \mathcal{R}_k = \mathcal{R}$.

These relations of the forward modeling and prior model is illustrated in the Figure 1.

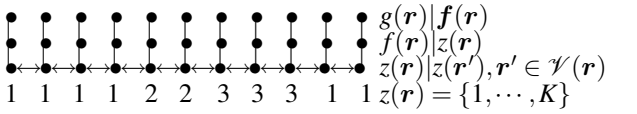

Figure 1: Proposed hierarchical model 1: $f(\boldsymbol{r})$ is a hidden variable for the data $g(\boldsymbol{r})$ and $z(\boldsymbol{r})$ is a hidden variable for the image $f(\boldsymbol{r})$.

However, in this model, we assumed that all the voxels $f(\boldsymbol{r})$ conditionally to $z(\boldsymbol{r})$ are independents. But, even if this hypothesis is valid for those voxels in different regions, this is not a valid one for the voxels inside a given region. To account for the Markov property of the voxels in a given region, we need to introduce a contour hidden variable $q(\boldsymbol{r})$ which is related to the classification hidden variable $z(\boldsymbol{r})$ by a deterministic relation $q(\boldsymbol{r}, \boldsymbol{r}') = \delta(z(\boldsymbol{r}) - z(\boldsymbol{r}'))$ where $\boldsymbol{r}'$ represents a position in the neighborhood $\mathcal{V}(\boldsymbol{r})$ of $\boldsymbol{r}$. With this new hidden variable, we can propose the following model:

$$p(\bar{f}(\boldsymbol{r})|q(\boldsymbol{r}, \boldsymbol{r}'), \bar{f}(\boldsymbol{r}'), \boldsymbol{r}' \in \mathcal{V}(\boldsymbol{r})) = \mathcal{N}\left(\bar{\bar{f}}(\boldsymbol{r}), \sigma_f^2\right) \quad (8)$$

where, again $\mathcal{V}(\boldsymbol{r})$ represents the six nearest neighbors of $\boldsymbol{r}$, $\bar{f}(\boldsymbol{r}) = \frac{f(\boldsymbol{r}) - m(\boldsymbol{r})}{\sqrt{v(\boldsymbol{r})}}$, $\quad \bar{\bar{f}}(\boldsymbol{r}) = \beta(\boldsymbol{r}) \sum_{\boldsymbol{r}' \in \mathcal{V}(\boldsymbol{r})} (1 - q(\boldsymbol{r}, \boldsymbol{r}'))\bar{f}(\boldsymbol{r})$

and $\quad \beta(\boldsymbol{r}) = \frac{1}{\sum_{\boldsymbol{r}' \in \mathcal{V}(\boldsymbol{r})}(1 - q(\boldsymbol{r}, \boldsymbol{r}'))}$.

This second model is illustrated in Figure 2.

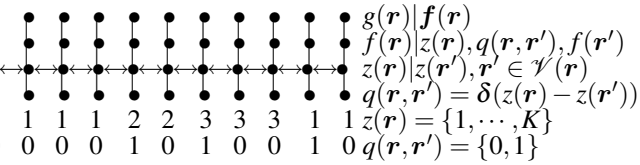

Figure 2: Proposed hierarchical model 2: $f(\boldsymbol{r})$ is a hidden variable for the data $g(\boldsymbol{r})$ and $z(\boldsymbol{r})$ and $q(\boldsymbol{r}, \boldsymbol{r}')$ are hidden variables for the image $f(\boldsymbol{r})$. Note that $q(\boldsymbol{r}, \boldsymbol{r}')$ is obtained from $z(\boldsymbol{r})$ in a deterministic way. Thus, we need only to estimate $z(\boldsymbol{r})$ from which we can deduce $q(\boldsymbol{r}, \boldsymbol{r}')$.

3. BAYESIAN ESTIMATION FRAMEWORK AND PROPOSED ALGORITHMS

Using the prior data model (3), the prior image models (5) or (8) and the prior Potts-Markov model (6) and also assigning appropriate prior probability laws $p(\underline{\theta})$ to the hyperparameters $\theta = \{\theta_\varepsilon, \theta_f\}$ where $\theta_\varepsilon = {\sigma_\varepsilon}^2$ and $\theta_f = \{(m_k, v_k)\}$, we obtain an expression for the posterior law

$$p(\boldsymbol{f}, \boldsymbol{z}, \theta | \boldsymbol{g}) \propto p(\boldsymbol{g}|\boldsymbol{f}, \theta_\varepsilon)\, p(\boldsymbol{f}|\boldsymbol{z}, \theta_f)\, p(\boldsymbol{z})\, p(\theta) \qquad (9)$$

In this paper, we used conjugate priors for all of them, *i.e.,* Gaussian for the means m_k and inverse Gamma for the variances v_k as well as for the noise variance ${\sigma_\varepsilon}^2$.

When given the expression of the posterior law, we can then use it to define an estimator such as Joint Maximum A Posteriori (JMAP) or the Posterior Means (PM) for all the unknowns. The first needs optimization algorithms and the second integration methods. Both are computationally demanding. Alternate optimization is generally used for the first while the MCMC techniques are used for the second.

3.1 Proposed algorithm

In this work, we propose to use the following iterative algorithm:

- Estimate $\boldsymbol{f}$ using $p(\boldsymbol{f}|\widehat{\boldsymbol{z}}, \widehat{\theta}, \boldsymbol{g})$ where

  $$p(\boldsymbol{f}|\boldsymbol{z}, \theta, \boldsymbol{g}) \propto p(\boldsymbol{g}|\boldsymbol{f}, \boldsymbol{z}, \theta)\, p(\boldsymbol{f}|\boldsymbol{z}, \theta)$$

  We may note that this conditional posterior law is Gaussian $p(\boldsymbol{f}|\boldsymbol{z}, \theta, \boldsymbol{g}) = \mathcal{N}(\widehat{\boldsymbol{f}}, \widehat{\Sigma})$. Then, we can write the expressions of the posterior mean $\widehat{\boldsymbol{f}}$ and covariance $\widehat{\Sigma}$. However, due to the operator $\boldsymbol{H}$, obtaining $\widehat{\Sigma}$ needs huge dimensional matrix inversion. For this reason, in this step, we obtain $\widehat{\boldsymbol{f}}$ by maximizing $p(\boldsymbol{f}|\widehat{\boldsymbol{z}}, \widehat{\theta}, \boldsymbol{g})$ or equivalently by minimizing $-\ln\, p(\boldsymbol{f}|\widehat{\boldsymbol{z}}, \widehat{\theta}, \boldsymbol{g})$:

  $$\widehat{\boldsymbol{f}} = \arg\min_{\boldsymbol{f}} \left\{ J(\boldsymbol{f}|\widehat{\boldsymbol{z}}, \widehat{\theta}, \boldsymbol{g}) = -\ln p(\boldsymbol{f}|\widehat{\boldsymbol{z}}, \widehat{\theta}, \boldsymbol{g}) \right\}$$

  where

  $$\begin{aligned} J(\boldsymbol{f}|\boldsymbol{z}, \theta, \boldsymbol{g}) &= \|\boldsymbol{g} - \boldsymbol{H}\boldsymbol{f}\|^2 + \lambda \sum_k \sum_{\boldsymbol{r} \in \mathscr{R}_k} \left| \frac{f(\boldsymbol{r}) - m_k}{\sqrt{v_k}} \right|^2 \\ &= \|\boldsymbol{g} - \boldsymbol{H}\boldsymbol{f}\|^2 + \lambda \sum_{\boldsymbol{r} \in \mathscr{R}} |\bar{f}(\boldsymbol{r})|^2 \qquad (10) \end{aligned}$$

  with $\bar{\boldsymbol{f}} = \left\{ \frac{f(\boldsymbol{r}) - m(\boldsymbol{r})}{\sqrt{v(\boldsymbol{r})}}, \boldsymbol{r} \in \mathscr{R} \right\}$ in the first model, and

  $$J(\boldsymbol{f}) = \|\boldsymbol{g} - \boldsymbol{H}\boldsymbol{f}\|^2 + \lambda \sum_{\boldsymbol{r} \in \mathscr{R}} \left| \bar{f}(\boldsymbol{r}) - \bar{\bar{f}}(\boldsymbol{r}) \right|^2 \qquad (11)$$

  with $\bar{\bar{f}}(\boldsymbol{r}) = \beta(\boldsymbol{r}) \sum_{\boldsymbol{r}' \in \mathscr{V}(\boldsymbol{r})} (1 - q(\boldsymbol{r}, \boldsymbol{r}'))\bar{f}(\boldsymbol{r}),$

  $q(\boldsymbol{r}, \boldsymbol{r}') = \delta(z(\boldsymbol{r}) - z(\boldsymbol{r}'))$ and $\beta(\boldsymbol{r}) = \frac{1}{\sum_{\boldsymbol{r}' \in \mathscr{V}(\boldsymbol{r})} (1 - q(\boldsymbol{r}, \boldsymbol{r}'))}$ in the second model. In both cases, $\lambda = {\sigma_\varepsilon}^2 / \sigma_f^2$ can be assimilated to a regularization parameter.

- Estimate $\boldsymbol{z}$ using $p(\boldsymbol{z}|\widehat{\boldsymbol{f}}, \widehat{\theta}, \boldsymbol{g}) \propto p(\boldsymbol{g}|\widehat{\boldsymbol{f}}, \boldsymbol{z}, \theta)\, p(\boldsymbol{z})$ where

  $$p(\boldsymbol{g}|\boldsymbol{f}, \boldsymbol{z}, \widehat{\theta}) = \mathcal{N}(\boldsymbol{H}\bar{\boldsymbol{f}}, \boldsymbol{H}\bar{\Sigma}\boldsymbol{H}' + \widehat{{\sigma_\varepsilon}^2}\boldsymbol{I})$$

  with

  $$\bar{\boldsymbol{f}} = \left\{ \frac{\widehat{f}(\boldsymbol{r}) - \widehat{m}(\boldsymbol{r})}{\sqrt{\widehat{v}(\boldsymbol{r})}}, \boldsymbol{r} \in \mathscr{R} \right\} \text{ and } \bar{\Sigma} = \text{diag}\,[\widehat{v}(\boldsymbol{r}), \boldsymbol{r} \in \mathscr{R}]\,.$$

- Estimate θ using $p(\theta|\widehat{\boldsymbol{f}}, \widehat{\boldsymbol{z}}, \boldsymbol{g})$ where

  $$p(\theta|\boldsymbol{f}, \boldsymbol{z}, \boldsymbol{g}) \propto p(\boldsymbol{g}|\boldsymbol{f}, {\sigma_\varepsilon}^2\boldsymbol{I})\, p(\boldsymbol{f}|\boldsymbol{z}, (m_k, v_k))\, p(\theta)$$

  where $\theta = \{{\sigma_\varepsilon}^2, (m_k, v_k)\}$. For the hyperparameters we choose conjugate priors, *i.e.,* the Gaussian for the means m_k and inverse Gamma for the variances ${\sigma_\varepsilon}^2$ and v_k. In this way, the corresponding posteriors are also Gaussian and Inverse Gamma. Their detailed expressions can be found in [10, 11, 12].

In this algorithm, by *estimate using* we mean either use the MAP or the posterior mean. For the first, we use an appropriate optimization algorithm and for the second an appropriate MCMC sampling technique.

To implement effectively this algorithm, we have to give details of its initialization which is an important task for its success. $\diamond$ **Initialization:**

- Initialize $z(\boldsymbol{r}) = 1$ and $q(\boldsymbol{r}) = 0, \forall \boldsymbol{r} \in \mathscr{R}$, ${\sigma_\varepsilon}^2 = 1, m_1 = 0$ and $\sigma_1^2 = 1$ and compute $\widehat{\boldsymbol{f}}$ by

  $$\widehat{\boldsymbol{f}} = \arg\max_{\boldsymbol{f}} \{p(\boldsymbol{f}|\boldsymbol{z}, \theta, \boldsymbol{g})\} = \arg\min_{\boldsymbol{f}} \{J(\boldsymbol{f})\}$$

  where

  $$J(\boldsymbol{f}) = \|\boldsymbol{g} - \boldsymbol{H}\boldsymbol{f}\|^2 + \lambda \sum_{\boldsymbol{r}\mathscr{R}} |f(\boldsymbol{r})|^2 \qquad (12)$$

  in the first model and

  $$J(\boldsymbol{f}) = \|\boldsymbol{g} - \boldsymbol{H}\boldsymbol{f}\|^2 + \lambda \sum_{\boldsymbol{r}\mathscr{R}} \left| f(\boldsymbol{r}) - \sum_{\boldsymbol{r}' \in \mathscr{V}(\boldsymbol{r})} f(\boldsymbol{r}') \right|^2 \qquad (13)$$

  in the second model.
  This step can be recognized as a classical minimum norm least squares (MNLS) or as a quadratic regularization (QR), or equivalently, as an i.i.d. Gaussian or a classical Gauss-Markov modeling solution which assume the whole image as one homogeneous region:
  $(K = 1, \quad z(\boldsymbol{r}) = 1, \quad q(\boldsymbol{r}) = 0, \quad \forall \boldsymbol{r} \in \mathscr{R})$.
- Then, fix K to a maximum number of possible materials in the object under the test, often $K = 2$ or $K = 3$, representing safe (metal), default (air) and intermediate (composite) and find a first estimate $\widehat{\boldsymbol{z}}$ for $\boldsymbol{z}$ using $p(\boldsymbol{z}|\widehat{\theta}, \widehat{\boldsymbol{f}}, \boldsymbol{g})$ which becomes

  $$p(\boldsymbol{z}|\widehat{\theta}, \widehat{\boldsymbol{f}}, \boldsymbol{g}) \propto \mathcal{N}(\boldsymbol{H}\bar{\boldsymbol{f}}, \boldsymbol{H}\boldsymbol{H}' + \boldsymbol{I})\; p(\boldsymbol{z})$$

  with $\bar{\boldsymbol{f}} = \widehat{\boldsymbol{f}}$. We note that $p(\boldsymbol{z}|\widehat{\boldsymbol{f}}, \widehat{\theta}, \boldsymbol{g})$ has the same Markov structure than $p(\boldsymbol{z})$ and getting a sample $\boldsymbol{z}$ from that can be obtained through a Gibbs sampling algorithm.
- Finally, given $\widehat{\boldsymbol{f}}$ and a first sample $\widehat{\boldsymbol{z}}$, obtain a first estimate for the hyperparameters ${\sigma_\varepsilon}^2$ and (m_k, v_k) by maximizing $p(\theta|\widehat{\boldsymbol{f}}, \widehat{\boldsymbol{z}}, \boldsymbol{g})$. The analytical expressions of these estimates can be obtained easily and are given in [11].

4. DISCUSSIONS

As we could see the initialization step of the proposed algorithm is equivalent to obtaining a first solution to the reconstruction problem via a quadratic regularization, or equivalently, via a Gauss-Markov prior modeling of the image. This step is crucial to the success of the method. In this initialization step, obtaining a first estimate for z and then for the hyperparameters is also crucial. In fact, here, we use effectively our prior knowledge about K the number of materials, and their means and variances. We can also use an EM algorithm in this step to obtain a better estimates of the MoG model by trying to fit this model to the histogram of the estimated voxels $\widehat{f}$ of the image.

5. SIMULATION RESULTS

In the following we show a few results obtained by simulating an experimental measurement system for a NDT application of metallic objects in a nuclear power plant. The introduced defects are for this study very simple defects (cubic form). Because of the great thickness of the pipe, the useful beams are contained within a very narrow angle (otherwise, the thickness to be crossed is too high); moreover, because of the limited room in the plant, it is impossible to revolve the pipe. In such conditions, we use seven positions for the source placed in the center of a circle and along the given circle. The radiographies angles are limited to about ± 15 degrees. Figure 3 shows such an experimental simulation data and result obtained with the classical backprojection method.

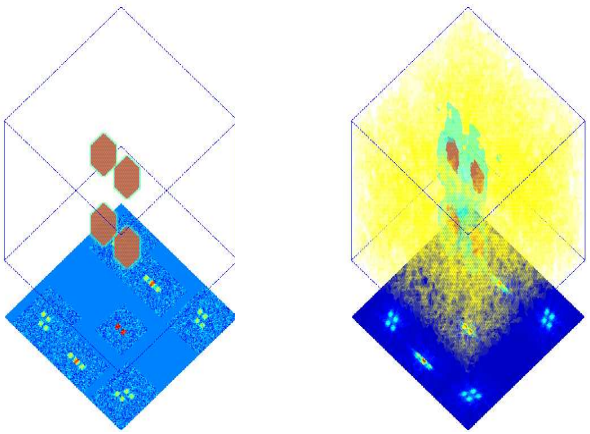

Figure 3: Simulated data and reconstruction result obtained with the classical backprojection method.

Figure 4 shows the reconstruction results which are obtained with the classical quadratic regularization method without and with positivity constraint and Figure 5 shows the reconstruction results obtained by the proposed methods.

6. CONCLUSIONS

A new method for tomographic image reconstruction from a small number of its limited angles projections is proposed. The originality of the proposed method is mainly using the Bayesian estimation approach with an appropriate hierarchical Markov model with a Potts Markov hidden variable which accounts for the specificity of the NDT applications. This work has been developed under a collaborative research work between CNRS and EDF. We plan now to study the sensitivity of the method to the acquisition parameters (source and films positions, blur, ...) and to apply it to real data in order to evaluate the full processing (digitization, calibration and reconstruction). This part of the work is under investigation in EDF research center in France.

REFERENCES

[1] Gabor T. Herman, H. K. Tuy, K. J. Langenberg, and P. C. Sabatier, *Basic Methods of Tomography and Inverse Problems*, Adam Hilger, Bristol, UK, 1987.

[2] Avinash C. Kak and Malcolm Slaney, *Principles of Computerized Tomographic Imaging*, IEEE Press, New York, NY, 1987.

[3] Stuart Geman and D. McClure, "Statistical methods for tomographic image reconstruction," in *Proceedings of the 46th Session of the* ICI, *Bulletin of the* ICI, 1987, vol. 52, pp. 5–21.

[4] Charles A. Bouman and Ken D. Sauer, "A generalized Gaussian image model for edge-preserving MAP estimation," *IEEE Trans. Image Processing*, vol. 2, no. 3, pp. 296–310, July 1993.

[5] L. Bedini, I. Gerace, and A. Tonazzini, "A deterministic algorithm for reconstructing images with interacting discontinuities," *Comput. Vision Graphics Image Process.*, vol. 56, no. 2, pp. 109–123, Mar. 1994.

[6] Stéphane Gautier, Jérôme Idier, Ali Mohammad-Djafari, and Blandine Lavayssière, "X-ray and ultrasound data fusion," in *Proc. IEEE ICIP*, Chicago, IL, Oct. 1998, pp. 366–369.

[7] Charles Soussen and Ali Mohammad-Djafari, "Polygonal and polyhedral contour reconstruction in computed tomography," *IEEE Trans. on Image Processing*, vol. 13, no. 11, pp. 1507–1523, Nov 2004.

[8] Mila Nikolova and Ali Mohammad-Djafari, "Eddy current tomography using a binary Markov model," *Signal Processing*, vol. 49, pp. 119–132, 1996.

[9] Mila Nikolova, Jérôme Idier, and Ali Mohammad-Djafari, "Inversion of large-support ill-posed linear operators using a piecewise Gaussian MRF," *IEEE Trans. Image Processing*, vol. 7, no. 4, pp. 571–585, Apr. 1998.

[10] Hichem Snoussi and Ali Mohammad-Djafari, "Fast joint separation and segmentation of mixed images," *Journal of Electronic Imaging*, vol. 13, no. 2, pp. 349–361, April 2004.

[11] Olivier Féron and Ali Mohammad-Djafari, "Image fusion and joint segmentation using an MCMC algorithm," *Journal of Electronic Imaging*, vol. 14(2), paper n023014, April 2005.

[12] Fabrice Humblot and Ali Mohammad-Djafari, "Super-resolution using hidden markov model and bayesian detection estimation framework," *To appear in EURASIP Journal on Applied Signal Processing*, vol. Special number on Super-Resolution Imaging: Analysis, Algorithms, and Applications, 2005.

[13] L. Fournier, L. Châtellier, B. Charbonnier and B. Chassignole, "3-D Reconstruction from narrow-angle radiographs," *QNDE*, 2004.

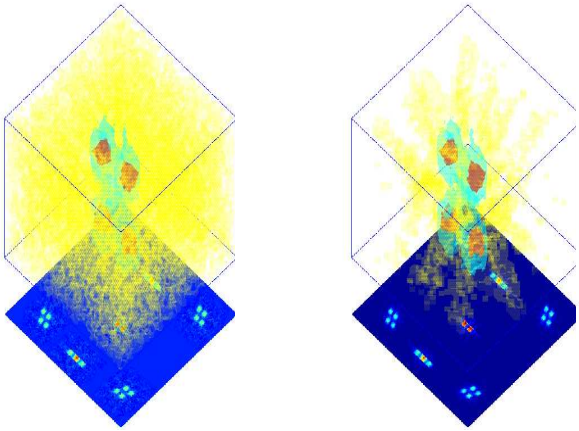

Figure 4: Reconstruction results obtained with the cla quadratic regularization method without and with pos and support constraint.

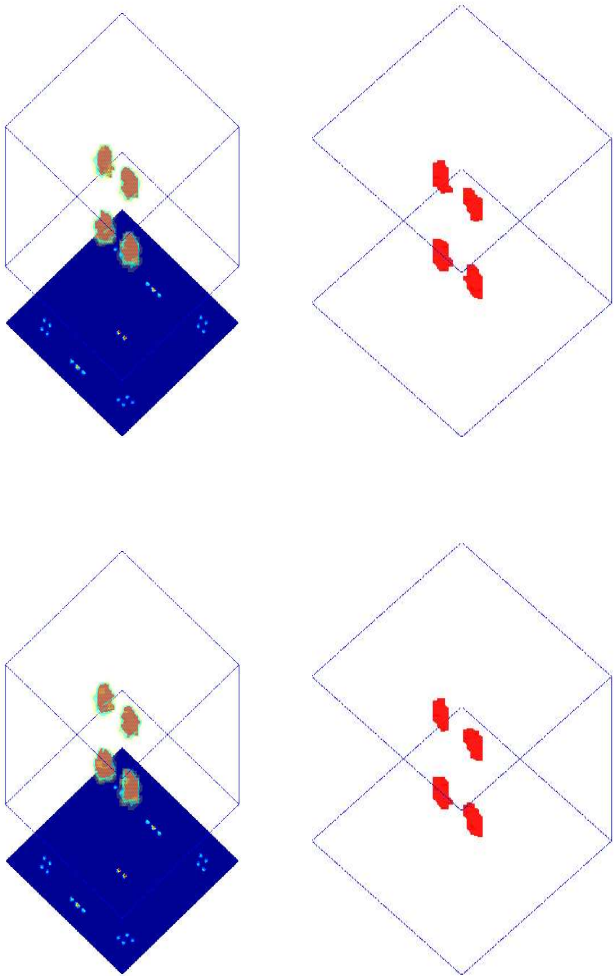

Figure 5: Reconstruction results obtained with the proposed methods: a) estimated intensity, b) estimated segmentation. Upper row: Method 1, Lower row: Method 2.